(5) Prigogine, I.; Defay, R. "Chemical Thermodynamics"; Longmans, Green and Co.: London, 1954.
(6) Patterson, D.; Delmas, G. *Discuss. Faraday Soc.*, **1970**, *49*, 98.
(7) Flory, P. J. *Discuss. Faraday Soc.* **1970**, *49*, 7.
(8) Rowlinson, J. S. "Liquid and Liquid Mixtures", 2nd ed.; Butterworth: London, 1969; p 167-170.
(9) Bailey, F. E.; Callard, R. W. *J. Appl. Polym. Sci.* **1959**, *1*, 56, 373.
(10) Bailey, F. E.; Kucera, J. L.; Imhof, L. G. *J. Polym. Sci.* **1958**, *32*, 517.
(11) Ring, W.; Cantow, H.-J.; Holtrup, W. *Eur. Polym. J.* **1966**, *2*, 151.
(12) Elias, H.-G.; Lys, H. *Makromol. Chem.* **1966**, *92*, 1.
(13) Liu, K.-J.; Parsons, J. *Macromolecules* **1969**, *2*, 529.
(14) Koenig, J.; Angood, A. *J. Polym. Sci., Polym. Phys. Ed.* **1970**, *8*, 1787.
(15) Eisenbach, C. D.; Peuscher, M. *Makromol. Chem., Rapid Commun.* **1980**, *1*, 105.
(16) Peuscher, M. Ph.D. Thesis, University of Freiburg, Freiburg, 1982.
(17) Ehl, P. J.; Loucheux, C.; Reiss. C.; Benoit, H. *Makromol. Chem.* **1964**, *75*, 35.
(18) Bortel, E.; Kochanowski, A. *Makromol. Chem., Rapid Commun.* **1980**, *1*, 205.
(19) Strazielle, C. *Makromol. Chem.* **1968**, *119*, 50.
(20) Nemethy, G.; Scheraga, H. A. *J. Phys. Chem.* **1962**, *66*, 1773; **1963**, *67*, 2888.
(21) Nemethy, G.; Scheraga, H. A. *J. Chem. Phys.* **1962**, *36*, 3382, 3401.
(22) Frank, H. S. In "Water: A Comprehensive Treatise"; Franks, F., Ed.; Plenum: New York, 1972; Vol. 1, Chapter 14.
(23) Tanford, C. "The Hydrophobic Effect"; Wiley: New York, 1973.
(24) Flory, P. J. "Principls of *Polymer Chemistry*"; Cornell University Press: Ithaca, NY, 1953.
(25) Tompa, H. "Polymer Solutions"; Butterworth: London, 1956.
(26) Godovsky, Yu. K.; Slonimsky, G. L.; Garbar, N. M. J. Polym. *Sci., Part C* **1972**, *38*, 1.
(27) Rayleigh, J. W. *Proc. R. Soc. London, Ser. A.* **1914**, *90*, 219.
(28) van de Hulst, H. C. "Light Scattering by Small Particles"; Wiley: New York, 1957.
(29) Kerker, M. "The Scattering of Light"; Academic Press: New York, 1969.
(30) Huglin, M. B. "Light Scattering from Polymer Solutions"; Academic Press: New York, 1972.
(31) Burchard, W. In "Applied Fibre Science"; Happey, F., Ed.; Academic Press: New York, 1978; Chapter 10.
(32) Burchard, W.; Kajiwara, K.; Nerger, D. *J. Polym. Sci., Polym. Phys. Ed.* **1982**, *20*, 157.
(33) Burchard, W., Thesis (Habilitation), University of Freiburg, Freiburg, 1966.
(34) Franks, F.; Asquith, M. H.; Hammond, C. C.; Skaer, H. L. B.; Echlin, P. *J. Microsc. (Oxford)* **1977**, *110*, 223.
(35) Bale, H. D.; Shepler, R. E.; Sorgen, D. K. *Phys. Chem. Liq.* **1968**, *1*, 181.
(36) Franks, F.; Asquith, M. H.; Hammond, C. C.; Skaer, H. B.; Echlin, P. *J. Micros. (Oxford)* **1977**, *110*, 223, 239.
(37) Dustin, P. "Microtubules"; Springer-Verlag; Heidelberg, 1978.
(38) Fraenkel-Conrad, H. "Chemie und Biologie der Viren"; G. Fischer Verlag: Stuttgart, 1974.
(39) Kjellander, K.; Florin, E. *J. Chem. Soc., Faraday Trans. 1* **1981**, *77*, 2053.
(40) Newman, S.; Krigbaum, W. R.; Laugier, C.; Flory, P. J., *J. Polym. Sci.* **1954**, *14*, 451.
(41) Muus, L. T.; Billmeyer, F. W. *J. Am. Chem. Soc.* **1957**, *79*, 5079.

Small-Angle Neutron Scattering Study of Block Copolymer Morphology

Randal W. Richards* and James L. Thomason†

Department of Pure and Applied Chemistry, University of Strathclyde, Glasgow G1 1XL, United Kingdom. *Received June 28, 1982*

ABSTRACT: Small-angle neutron scattering has been used to investigate the structural features of styrene–isoprene block copolymers. A wide range of molecular weight and composition has been investigated, encompassing the spherical, cylindrical, and lamellar morphologies of styrene domains chiefly. Apart from domain separation and packing, domain size has been determined by using copolymers with fully deuterated styrene blocks to improve contrast. While domain sizes are in some agreement with statistical thermodynamic theory no such agreement is found for domain separation. Possible reasons for this are discussed, especially for those copolymers with spherical morphology. Results also indicate that thermal annealing of the copolymers increases the grain size rather than improving the packing of domains with respect to each other.

Introduction

Structural investigations of the polymeric solid state over large length scales have used the techniques of electron microscopy and small-angle X-ray scattering (SAXS). Each of these suffers from disadvantages that make them unsuitable for studying structure over the range from supramolecular organization down to individual polymer molecules. Electron microscopy (EM) requires thin samples which have to be stained or replicated to produce observable images and this process may produce artifacts.[1] SAXS also requires thin samples (but not so thin as in EM); additionally, contrast in this technique relies on a good electron density difference between the matrix and the species being investigated,[2] and for many organic polymers the electron density difference cannot be enhanced sufficiently without drastic chemical modifications. Small-angle neutron scattering (SANS) is a relatively new technique[3-6] for the investigation of polymer structure and supramolecular organization but has produced definitive data for the critical evaluation of molecular theories of polymer structure and has contributed much to the debate on crystalline polymer structure.[7] The greater contribution of SANS in such a short time arises from the large neutron scattering cross section of hydrogen atoms and the considerable difference in scattering cross section for hydrogen and deuterium atoms. It is this difference that generates a contrast enabling "individual molecules" to be observed and their dimensions measured. The majority of work published thus far deals with the use of SANS in the determination of radii of gyration in homogeneous polymer systems. It is only recently that extensions to heterogeneous systems have been attempted. Styrene–diene block

† Present address: Institut für Physikalische Chemie, Universität Mainz, D6500 Mainz, West Germany.

0024-9297/83/2216-0982$01.50/0

copolymers are a particularly interesting example of heterogeneous polymers in that the phase-separated structure displays regularity over large length scales (thousands of angstroms) while the morphology of the phase-separated structures depends on the composition.[8-10] Numerous SAXS investigations[11-16] have been reported on styrene–diene copolymers and statistical thermodynamic theories of varying degrees of detail have been published.[17-20] Apart from the recent work of Hashimoto et al.[21,22] there appears to have been no concerted study of all three morphologies over a range of copolymer molecular weights. A detailed study of the lamellar phase has been reported by Skoulios and Hadziioannou,[23] but here the materials were deliberately prepared to have a "single-crystal" type texture, which is only obtained under special circumstances.

We have been examining styrene–isoprene block copolymers using SANS with the aim of characterizing the structural organization down to the submolecular level and making full use of the advantages of selective deuteration. Preliminary results have been published elsewhere[24] for a limited range of copolymers. A fuller examination of domain morphology and separation as a function of molecular weight is presented here and the results are compared with SAXS data, where appropriate, and the predictions of current theory.

Experimental Section

Copolymer Preparation and Characterization. Diblock (SI) and triblock (SIS) copolymers of styrene and isoprene were prepared by sequential anionic polymerization using *n*-butyllithium as initiator; the detailed procedure and the apparatus used have been previously described.[25] Copolymers with deuterated styrene blocks (prefixed D) were also prepared in a similar manner with styrene-d_8 supplied by Aldrich Ltd.

All copolymers were analyzed by gel permeation chromatography using UV detection; additionally, the number-average molecular weights ($\bar{M}_n$) of the hydrogenous copolymers in benzene were measured by membrane osmometry with a Knauer recording membrane osmometer. Number-average molecular weights for DSI and DSIS copolymers were not determined in this way due to the small quantities available. Small samples of the polystyrene homopolymer were retained for the determination of domain molecular weight, M_D, by GPC.

The weight fraction of styrene in the copolymers was determined by UV spectroscopy on solutions made up in spectroscopic grade chloroform. Absorbance over the wavelength range 275–250 nm was scanned, the maxima for polystyrene at 262 and 268 nm being used for analysis purposes. Additionally, styrene weight fractions were also determined by combustion analysis as a confirmation of the UV analysis.

A detailed examination of the polyisoprene microstructure was not performed; however, since the polymerizations were carried out in benzene, the microstructure should mainly be that due to cis-1,4 addition. A comparison of the infrared spectra of polyisoprene homopolymer, produced under conditions identical with those used for the copolymers, and the copolymers with published spectra of polyisoprenes with varying microstructure[26] leads us to conclude that the microstructure of the polyisoprene chains is ca. 90% cis-1,4 addition and 5% 3,4 addition.

Electron Microscopy. Ultrathin sections were microtomed from the solution-cast copolymer films used for SANS (see below). For this purpose small samples were cut from the main specimen and hardened chemically by exposure to osmium tetraoxide vapor for 2 days. The sections were then cut by using an LKB 2088 ultramicrotome, the specimen temperature being 173 K while the glass knife temperature was 233 K. Sections were floated onto 50% v/v aqueous dimethyl sulfoxide solution, where they were picked up onto standard electron microscopy grids. After they were washed with distilled water and dried, the sections were exposed to osmium tetraoxide vapor for a further 15 min to ensure that the isoprene domains were stained. Transmission electron microscopy was performed with a Phillips EM200 electron microscope at an operating voltage of 80 kV. Measurements of the domain size and separation from the micrographs were made by using a 10-fold magnifying eyepice and graticule.

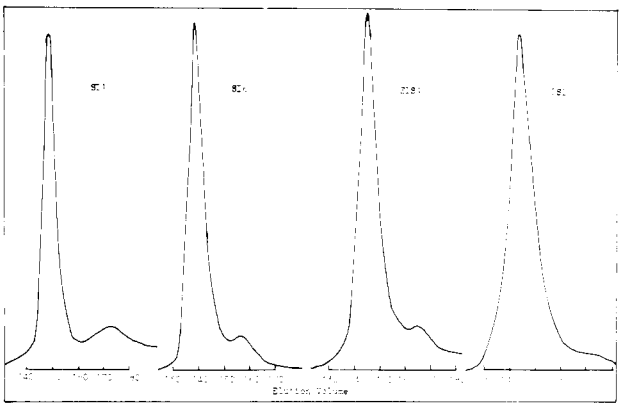

Figure 1. Typical gel permeation chromatograms of block copolymers.

Small-Angle Neutron Scattering. Sample Preparation. Copolymer films were cast from toluene solutions directly onto optical-quality quartz disks, with a diameter of 20 mm, which were mounted in a purpose-designed PTFE casting block. The solutions, generally ca. 8% w/v copolymer, were left to evaporate slowly over a period of 1 week; thereafter the disks were placed in a vacuum oven at room temperature for a further week or more to remove the last traces of solvent. Generally, the thickness of the copolymer films so prepared was in the region of 0.5 mm.

Small-Angle Neutron Diffractometers. SANS measurements on the copolymer samples were made at room temperature with three instruments, the small-angle spectrometer at AERE Harwell, U.K., and the D11 and D17 diffractometers on the high-flux beam reactor at the Institut Laue-Langevin, Grenoble, France. The instrumental features of each diffractometer are similar, the major differences being in the neutron flux incident on the samples and the range of scattering vector, Q, available to each instrument. Descriptions are available in the literature.[27,28] The range of neutron wavelengths (λ) used was $5 < \lambda < 16$ Å and the range of Q investigated was $3 \times 10^{-3} < Q < 0.18$. Å^{-1} Background scattering from the quartz disk was subtracted from each experimental measurement and the data were normalized to the scattering from a calibrant. Water was used for this purpose and generally a 2-mm path length quartz cell was used to contain it. This data correction and normalization was performed by using analysis programs developed by Dr. R. E. Ghosh at the Institute Laue-Langevin.[29]

Results

Copolymer Characterization. The accuracy of the UV analysis of the copolymers was checked by repeating the analysis on mixtures of polystyrene and polyisoprene of known composition; the agreement was excellent. Repeated analysis of the copolymer samples showed that results were reproducible. Typical GPC chromatograms for deuterated and hydrogenous copolymers are reproduced in Figure 1. Generally, molecular weights are obtained from GPC chromatograms by using the "universal calibration" procedure, which relies on having accurate values for the Mark–Houwink parameters, K and α, for both calibrant polymers and the unknowns.[30] These parameters are not available for styrene–isoprene block copolymers covering the composition range studied here. Another approach is to use the weighted average of log (molecular weight) values as suggested by Runyon et al.[31] and supported by the detailed examination of Tung.[32] In this method the copolymer molecular weight is given by

$$\log M_{CP} = W_S \log M_S + (1 - W_S) \log M_I$$

where M_{CP} is the molecular weight of the copolymer, W_S is the styrene weight fraction, and M_S and M_I are the molecular weights of the styrene and isoprene homopolymers, which have the same GPC elution volumes as

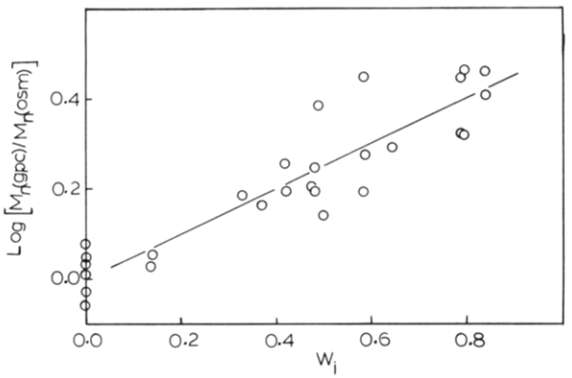

Figure 2. Number-average molecular weight ratios plotted as a function of isoprene weight fraction, W_I, according to eq 1.

the copolymer. Tung has shown that the molecular weight of polyisoprene determined by GPC, M_I^*, is related to the true molecular weight by a relationship of the form

$$M_I^* = kM_I$$

and for calibration using polystyrenes with THF as solvent, $k = 1.35$. Consequently, the equation for the copolymer molecular weight is rewritten as

$$\log M_{CP}^* = W_S \log M_S + (1 - W_S) \log M_I^*$$

where M_{CP}^* is the molecular weight of the copolymer obtained from the polystyrene calibration curve. This equation can be rearranged to give

$$\log M_{CP}^* = W_S \log M_S + (1 - W_S) \log M_I + (1 - W_S) \log k = \log M_{CP} + (1 - W_S) \log k$$

where M_{CP} is the true copolymer molecular weight; hence,

$$\log (M_{CP}^*/M_{CP}) = (1 - W_S) \log k \quad (1)$$

A plot of the ratio of number-average values from GPC and osmometry using data for hydrogenous copolymers as a function of W_I is shown in Figure 2. The slope of the best-fit straight line gives $k = 3.2$, which is somewhat higher than the value of 1.35 quoted by Tung and may be due to our usage of copolymer molecular weights determined by two different methods whereas Tung has used homopolymer molecular weights. In view of this dependence of M_{CP} on copolymer composition, number-average molecular weights from osmometry have been used throughout. For the deuterated block copolymers these values were not available from experimental measurements but have been calculated from eq 1 by using the GPC value of $\bar{M}_n$ and $k = 3.2$ as determined above. Copolymer molecular weights are given in the separate sections below; polydispersity ratios (from $\bar{M}_w/\bar{M}_n$) determined from GPC molecular weight averages are also included.

Electron Microscopy. Representative electron micrographs are shown in Figure 3 for lamellar and cylindrical styrene domain morphologies. Copolymers with spherical styrene domain morphology were more difficult to examine by electron microscopy primarily due to the heavy staining by the osmium tetraoxide, which apparently contaminated the styrene domains, thereby reducing the contrast. The micrographs show that the domains are highly organized on a local scale, with cylindrical domains exhibiting perfect hexagonal close packing (hcp). At a longer range it is clear that the copolymers have "grains" which are oriented at different angles to the incident electron beam. This is most evident for the cylindrical domains (Figure 3c,d) but is also clearly shown by the lamellar domains of Figure 3a, where the lamellar domains in the grains run almost orthogonal to each other.

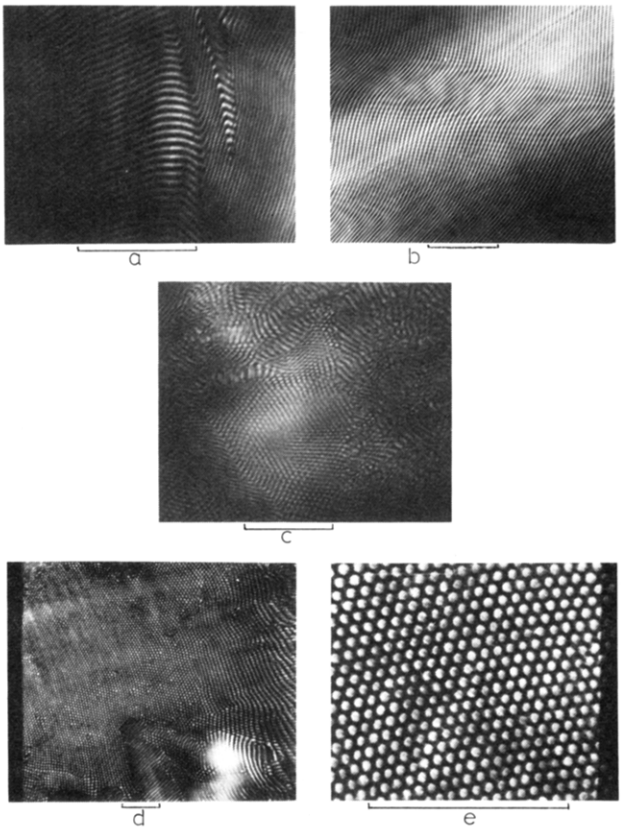

Figure 3. Electron micrographs of block copolymers: (a) SI8; (b) SI3; (c) SI2; (d) DSI6; (e) DSI6. Marker indicates a length of 1 μm.

Table I
Interdomain Separation and Domain Size from Electron Micrographs

(a) Lamellar Morphology

copolymer	d, Å	L_{PS},[a] Å
SI3	555 ± 10	293 ± 80
SI4	1025 ± 160	653 ± 67
SI6	564 ± 16	242 ± 29
SI7	315 ± 15	133 ± 26
SI8	558 ± 235	393 ± 73
SI9	1075 ± 446	480 ± 80
SIS3	413 ± 70	198 ± 35
DSI9	313 ± 11	130 ± 23
DSI11	534 ± 10	312 ± 9

(b) Cylindrical Morphology

copolymer	d, Å	R_C, Å
SI2	575 ± 113	183 ± 32
SI5	1083 ± 208	332 ± 26
DSI5	724 ± 206	186 ± 46
DSI6	744 ± 109	256 ± 24
DSI10	643 ± 72	265 ± 20

(c) Spherical Morphology

copolymer	d, Å	R_S, Å
SI1	406 ± 48	141 ± 8
SIS1	454 ± 37	108 ± 6
DSI1	449 ± 52	129 ± 10
DSIS1	390 ± 70	87.5 ± 8
ABC1	359 ± 14	131 ± 12

[a] Polystyrene lamellar thickness.

For each of the copolymers that were able to be investigated by transmission electron microscopy, the interdomain separation, d, and the domain size were measured optically; Table I gives the spread of values noted for each morphology.

Table II
Scattering Lengths (SL), Scattering Length Densities (D_{SL}), and Incoherent Scattering Cross Sections (CS_{IS}) for Nuclei and Scattering Units in Block Copolymers

SC[a]	SL, cm	D_{SL}, cm cm^{-3}	CS_{IS}, cm^2
^{1}H	-0.374×10^{-12}		81.5×10^{-24}
^{2}H	0.667×10^{-12}		7.6×10^{-24}
^{12}C	0.665×10^{-12}		5.5×10^{-24}
C_8H_8		1.416×10^{10}	696.0×10^{-24}
C_8D_8		6.302×10^{10}	104.8×10^{-24}
C_6H_8		0.289×10^{10}	679.5×10^{-24}

[a] Scattering center.

Small-Angle Neutron Scattering. The scattering of neutrons by neutron–nucleus interaction has two components, one termed coherent and the other incoherent.[4] Only the coherent scattering retains phase factors and therefore contains information on the structure of the scattering substance. The incoherent elastic scattering is isotropic and contains no structural information since the intensity of this type of scattering is independent of angle; in effect it constitutes a flat background scattering to the coherent scattering. Coherent scattering arises from two sources, the scattering length density of the scattering centers and any correlations between scattering centers. Incoherent scattering arises from the incoherent scattering cross section of the scattering centers. Table II gives scattering lengths and incoherent scattering cross sections for ^{12}C, ^{1}H, and ^{2}H nuclei plus the scattering length densities and incoherent scattering cross sections for the monomer units that act as the scattering centers in the copolymers. Consequently the total scattered neutron intensity at a scattering vector $\mathbf{Q}$, $I(\mathbf{Q})$, is given by[25,33]

$$I(\mathbf{Q}) = I_0 S t \exp(-n_n \sigma_t t) n_n \left(\frac{d\sigma_c}{d\Omega} + \frac{\sigma_{inc}}{4\pi} \right) \epsilon \Delta\Omega \quad (2)$$

where I_0 is the incident neutron beam intensity with cross sectional area S on a sample with thickness t, an average nuclear density n_n, a total scattering cross section σ_t, and an incoherent scattering cross section σ_{inc}. The detector efficiency is ϵ, while $\Delta\Omega$ is the solid angle in which neutrons are counted. In this equation the important term for structural purposes is $d\sigma_c/d\Omega$, the differential coherent scattering cross section per atom. The instrumental factors I_0, S, ϵ, and $\Delta\Omega$ can be normalized out by dividing the measured intensity by that of a material which scatters purely incoherently, water being used most often for this purpose; additionally $\exp(-n_n\sigma_t t)$ is the sample transmission. Considering the differential coherent scattering cross section, this can be written down in general terms by using a two-phase model,[33] i.e., N_p scattering particles of volume V_p and scattering length density ρ_p dispersed in a matrix of scattering length density ρ_p

$$d\sigma_c/d\Omega = (N_p V_p^2/N) \times (\rho_p - \rho_m)^2[(\langle F_p^2(\mathbf{Q})\rangle - \langle F_p(\mathbf{Q})\rangle^2) + \langle F_p(\mathbf{Q})\rangle^2 A(Q)] \quad (3)$$

where N is the number of nuclei in the beam, $F_p(\mathbf{Q})$ is the single-particle form factor (SPFF), and $A(Q)$ is a function describing the scattering due to interparticle interference effects. For block copolymers the particles will be in the first instance the domains and assuming they are reasonably uniform in shape and size, then $\langle F_p^2(\mathbf{Q})\rangle \approx \langle F_p(\mathbf{Q})\rangle^2$, and eq 3 reduces to

$$d\sigma_c/d\Omega = (N_p V_p^2/N)(\rho_p - \rho_m)^2 \langle F_p(\mathbf{Q})\rangle^2 A(Q) \quad (4)$$

The detailed form of the interference function is not known (indeed it is one of the parameters investigated here) but it can be assumed to possess the features of the structure factor for liquids; i.e., beyond a certain critical value of $\mathbf{Q}$ it reduces to a value of 1.

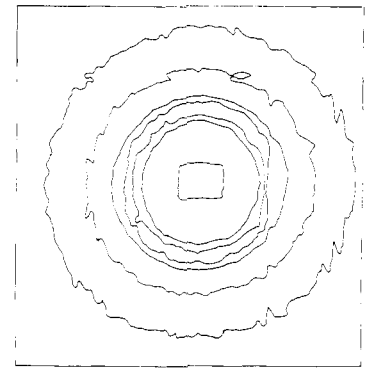

Figure 4. Contour plot of SANS intensity from DSIS2.

Hence the total scattered neutron intensity is

$$I(\mathbf{Q}) = k n_n (N_p V_p^2/N)(\rho_p - \rho_m)^2 \langle F_p(\mathbf{Q})\rangle^2 A(Q) + k n_n (\sigma_{inc}/4\pi) \quad (5)$$

Equation 5 is the formula that embodies the description of the scattering at the beginning of this section. The flat isotropic background is evident in the second component on the right-hand side of eq 2. The first term has all the structural information; below the critical Q value discussed above, $A(Q)$ is evident as a series of discrete peaks in the diffraction profile ($I(\mathbf{Q})$ as a function of Q). Above the critical value of Q, the shape of the scattering envelope is determined by $\langle F_p(\mathbf{Q})\rangle^2$, which in turn is determined by the domain morphology and the contrast factor, $(\rho_p - \rho_m)^2$. An additional factor that should be present in eq 2 for a complete description of the scattered neutron intensity is the orientation distribution function of the grains, containing many domains, with respect to the incident neutron wave vector. This factor should not be of significance for spherical domain morphology but may be of importance for lamellar and cylindrical domain morphology if there is a preferred grain orientation. The function describing this orientation distribution for lamellar and cylindrical domain morphologies will be composed of two angles describing grain orientation with respect to the incident neutron wave vector and this should be convoluted with the first term on the right-hand side of eq 2. Examination of electron micrographs indicates that grain orientation over the area of sample illuminated by the beam ($\sim$1 cm^2) is completely random. If this is the case then the scattering due to the interference function should appear as a series of Debye–Scherrer rings, since the block copolymer would be akin to a "polycrystalline" aggregate for small-angle scattering purposes. Figure 4 shows a contour plot for a triblock copolymer with spherical morphology, where the lines connect points of equal intensity on the detector. The intensity is radially isotropic about the center and is thus in agreement with the idea that the grains are randomly distributed. Diffraction profiles were therefore obtained from the radical average aroung the incident wave vector.

Equation 2 shows that, in principle, information on domain separation and arrangement is obtainable from $A(Q)$, while at higher Q values the domain size may be calculated since the scattering should have the characteristics of the SPFF pertaining to the domain morphology. These two aspects are discussed separately for the three domain morphologies.

1. Domain Separation and Arrangement. Lamellar Morphology. Table III gives the molecular weight and composition of those copolymers with lamellar morphology,

Table III
Characterization and SANS Data for Block Copolymers with Lamellar Morphology

sample	W_S	$10^{-3}\bar{M}_n$ copolymer	$\bar{M}_w/\bar{M}_n$	d, Å	$10^{-3}\bar{M}_w$ domain	L, Å
SI3	0.685	143.50	1.09	739	52.67	400
SI4	0.728	178.10	1.06	952	91.98	572
SI6	0.527	132.21	1.11	714	79.37	376
SI7	0.578	37.77	1.13	310	26.70	180
SI8	0.527	105.30	1.07	587	80.54	308
SI9	0.514	86.43	1.06	776	92.15	414
SIS3	0.505	121.20	1.14	459	25.55	210
DSI7	0.482	16.72	1.50	226	12.79	112
DSI9	0.574	32.63	1.61	326	22.751	186
DSI11	0.531	59.33	1.09	511	42.15	240

Table IV
Characterization and SANS Data for Block Copolymers with Cylindrical Morphology

sample	W_S	$10^{-3}\bar{M}_n$ copolymer	$\bar{M}_w/\bar{M}_n$	d, Å	$10^{-3}\bar{M}_w$ domain	R_C, Å
SI2	0.355	70.06	1.15	678	37.32	220
SI5	0.850	292.50	1.39	1577	105.00	355
SIS4	0.620	105.30	1.11	460	21.80	140
DSI3	0.398	114.08	1.58	1067	83.21	315
DSI5	0.817	99.57	1.34	776	35.50	185
DSI6	0.545	132.43	1.49	874	102.30	320
DSI10	0.428	81.21	1.29	626	51.29	218

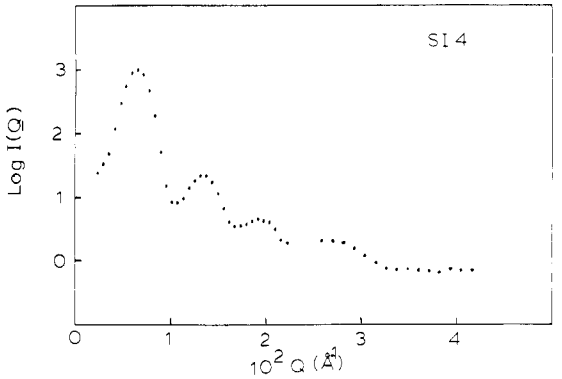

Figure 5. SANS diffraction profile for SI4.

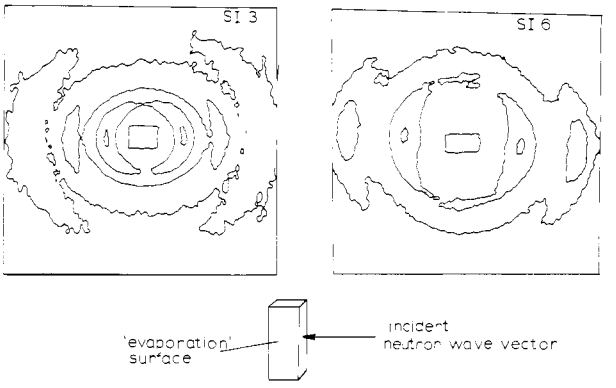

Figure 6. Contour plots for lamellar copolymers with incident wave vector parallel to the evaporation surface.

while Figure 5 shows a typical diffraction profile. A well-resolved main peak is clearly evident, with subsidiary peaks at higher Q becoming less well resolved as Q increases. This decrease in resolution is in part due to the interference function approaching the value of 1 but is also attributable to the instrumental resolution becoming poorer at the higher Q values; this aspect is more clearly shown in the discussion on cylindrical domains below. From electron microscopy and small-angle x-ray scattering studies of lamellar block copolymers by other workers, it has been stated that the lamellae are arranged parallel to the "evaporation" surface of solution-cast specimens.[21] It is clear from our electron micrographs and the fact that diffraction maxima are evident for our specimens where the incident wave vector is normal to the evaporation surface that this statement cannot be entirely true. Some experiments were made with the incident neutron wave vector parallel to the evaporation surface, and contour plots for two such measurements are shown in Figure 6. It is apparent that there is a preference for lamellar domains to be parallel to the evaporation surface as shown by the high-intensity arcs in the meridional direction. However, these arcs have a large degree of extension around the radius. The Q value of the maxima in the diffraction profiles was identical within the resolution of the diffractometer whether the incident wave vector was parallel or perpendicular to the "evaporation" surface of the polymer film. Because of this and due to the difficulty of mounting strips "edge on" to the beam such that additional orientation distribution was avoided, all data reported here are for incident wave vectors normal to the copolymer film "evaporation" surface. The diffraction profiles thus obtained had at least four maxima evident and in one case up to the ninth-order diffraction maxima were present. Bragg's law was used to calculate the spacings corresponding to these maxima, i.e.,

$$d_i = 2\pi/Q_i$$

For a perfectly lamellar array then, d_i/d_1 should have the values 1, 0.5, 0.33, 0.25, 0.2, 0.167, etc. for i increasing from 1. This relationship was always strictly obeyed by the first three Bragg maxima but in some cases maxima at higher Q were absent. These absences are discussed in a later section. Interdomain separations, the spacing from the midpoint of one styrene lamella to the next, obtained as d values are given in Table III.

Cylindrical Morphology. Molecular weights and compositions of those block copolymers with cylindrical domains are given in Table IV; a typical diffraction profile obtained on the D11 diffractometer at the Institut Laue-Langevin is shown in Figure 7. Again one maximum of large amplitude is followed by several at higher Q and with lower amplitude, in some cases there is a suggestion of double maxima being present. Included in this figure are data for the same copolymer obtained on the same dif-

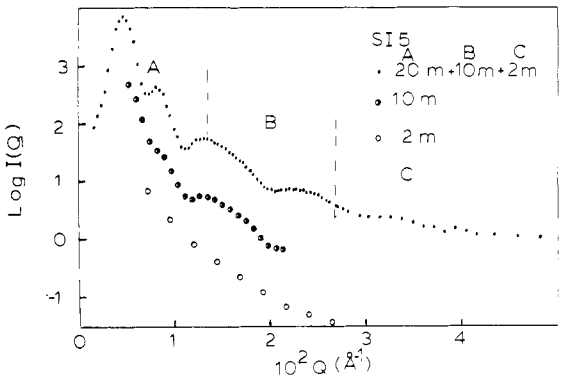

Figure 7. Diffraction profiles for SI5 obtained at the different sample–detector distances indicated.

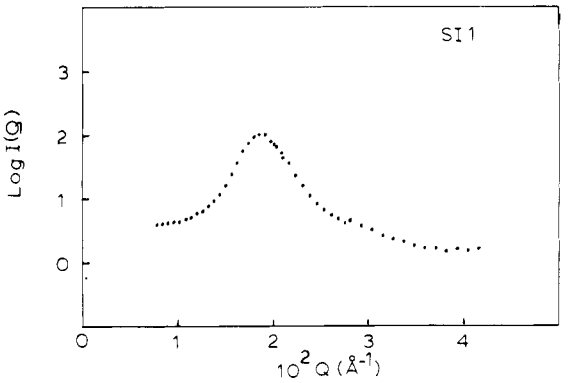

Figure 8. Diffraction profile for SI1.

fractometer at overlapping Q ranges (different sample–detector distances). For clarity, the data have been shifted on the intensity scale with respect to each other. The decrease in resolution at the higher Q ranges is clearly evident since much of the detail of the diffraction maxima is lost. For cylinders arranged as a hexagonally close packed array, the spacings calculated from the Bragg maxima are associated with the separation of particular lattice planes, which are characterized by Miller indices hk. The peak of largest amplitude is that due to the 10 plane and the ratio $d_{hk}/d_{10} = [1/(h^2 + hk + k^2)]^{1/2}$; values for this ratio have been tabulated earlier,[24] and assignment to an hcp structure was made on the basis of agreement of experimental ratios with these theoretical values. Interdomain separations, d, quoted in Table IV have been calculated as $2/3^{1/2}$ times the 10 plane spacing calculated from the diffraction maximum. It is evident from the composition figures quoted in Table IV that for $W_S < 0.5$ the cylindrical domains are composed of styrene, while above this value the cylinders are formed by the isoprene blocks. We are somewhat puzzled by DSI6 and DSI10 having cylindrical morphology since their compositions would a priori suggest a lamellar structure. However, the SANS diffraction profiles and the electron micrographs both show clear evidence for cylindrical styrene domains. Repeated measurements on these copolymers with samples prepared at different times always produced the same morphology. This departure from the predicted equilibrium morphology may be due to the polydispersity of the copolymers, but other factors could also be responsible, e.g., solvent evaporation rate.

Spherical Morphology. Diffraction profiles from styrene–isoprene block copolymers with spherical morphology were not as detailed as those from the lamellar or cylindrical morphologies. In part this is due to the molecular weights being relatively low, which places the diffraction maxima in a low-resolution Q range. A typical diffraction profile is shown in Figure 8, usually it was possible to discern at least two weak higher order diffraction maxima. There is not sufficient detail in the diffraction profiles from copolymers with spherical morphology to define uniquely a particular arrangement. The simplest options are simple cubic (scub), body-centered cubic (bccub), and faced-centered cubic (fccub). The best agreement between experimental and calculated volume fractions (vide infra) is obtained by using an fccub structure and consequently all the interdomain separations reported herein are calculated on this basis as $(3/2)^{1/2}$ of the interplanar spacing.

2. Domain Size. It was noted earlier that above a critical value of Q, the interference function is reduced to 1 and the coherent scattering law is determined by the

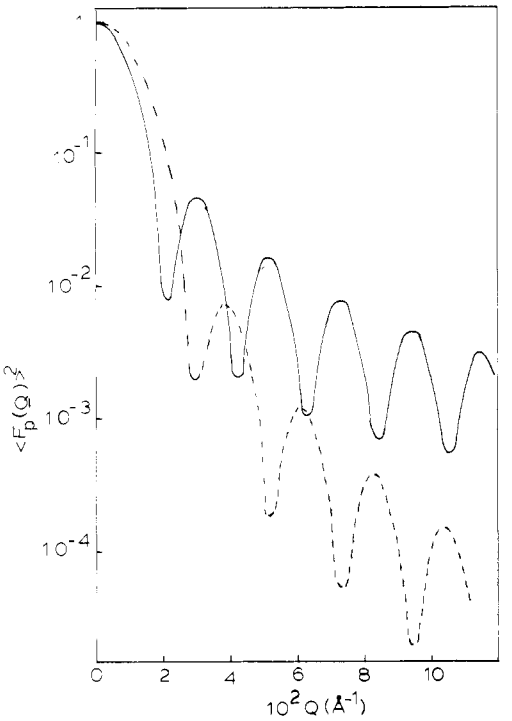

Figure 9. Single-particle form factor behavior as a function of Q for a lamella of thickness 300 Å (—) and a sphere of radius 150 Å (- - -).

SPFF, $\langle F_p(\mathbf{Q})\rangle^2$. For the three morphologies encountered in these block copolymers the SPFF's are determined by Bessel functions, J_n, of different order n:

for lamellae

$$\langle F_p(\mathbf{Q})\rangle^2 = \frac{\pi}{2(QL/2)} J_{1/2}{}^2(QL/2)$$

where L is the lamellar thickness,

for cylinders

$$\langle F_p(\mathbf{Q})\rangle^2 = 4J_1{}^2(QR_C)/(QR_C)^2$$

where R_C is the cylinder radius, and

for spheres

$$\langle F_p(\mathbf{Q})\rangle^2 = \frac{9\pi}{2(QR_S)^3} J_{3/2}{}^2(QR_S)$$

where R_S is the sphere radius. Figure 9 shows the behavior of the two extremes of $\langle F_p(\mathbf{Q})\rangle^2$, i.e., for lamellae and spherical particles. The major feature of all the SPFF's is a series of maxima of decreasing amplitude with increasing scattering vector Q. The Q values of the maxima

Table V
Characterization and SANS Data for Block Copolymers with Spherical Morphology

sample	W_S	$10^{-3}\bar{M}_n$ copolymer	$\bar{M}_w/\bar{M}_n$	d, Å	$10^{-3}\bar{M}_w$ domain	R_S, Å
SI1	0.203	30.55	1.07	414	11.23	130
SIS1	0.153	34.72	1.17	397	9.67	118
SIS2	0.413	50.00	1.07	376	19.10	151
DSI1	0.329	62.18	1.06	469	21.07	173
DSIS1	0.12	46.12	1.08	308	5.62	73
DSIS2	0.34	68.67	1.07	521	29.10	190
ABC1	0.212	86.00	1.06	557	27.87	175

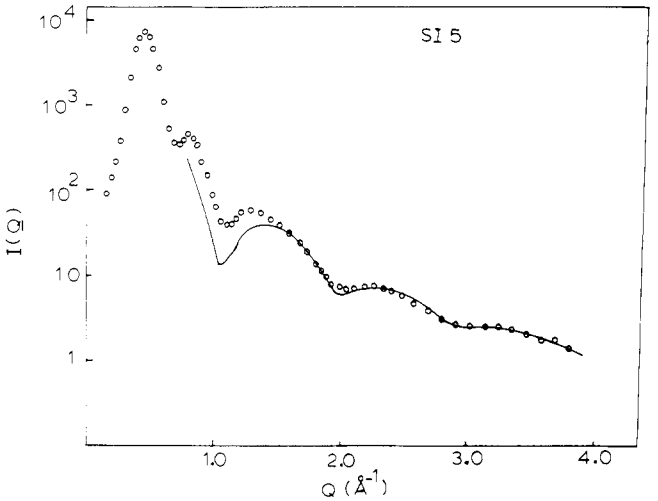

Figure 10. Example of fit of theoretical SPFF to the diffraction profile of SI5 in the intermediate Q region: Experimental (○); theoretical (—).

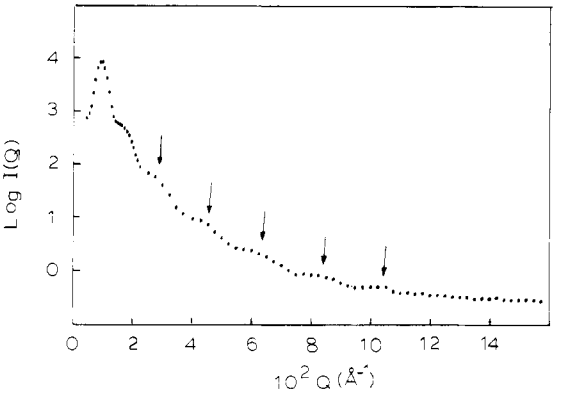

Figure 11. Diffraction profile for DSI5 in the intermediate Q region. Arrows indicate positions of single-particle form factor maxima.

enable the determination of the domain size since they occur at defined values of $Q(L/2)$, QR_C, or QR_S no matter what the domain dimensions are. These features are observable in the intermediate Q range, where the interference function, $A(Q)$, does not contribute markedly to the observed scattering. However, in this region the counting statistics are much worse than in the lower Q region and as noted earlier the resolution is poorer. Improvements in statistics were gained by counting for long times, and by very careful inspection of diffraction profiles in the intermediate Q range it was possible to identify sufficient maxima for the hydrogenous copolymers to give the domain dimensions in Tables III–V. Figure 10 shows the fit obtained in this region by use of a theoretical equation based on eq 5. It was to improve the accuracy in these measurements that copolymers with deuterated styrene blocks were prepared. Referring to eq 5, we note that the scattered intensity is controlled by the contrast factor, $(\rho_p - \rho_m)^2$; consequently by increasing this factor, we hoped that the oscillations at intermediate Q would become more apparent. Figure 11 shows the scattering profile in the intermediate Q range for DSI5, which clearly shows a number of broad maxima. However, there is no dramatic improvement in the ability to discern the maxima compared to purely hydrogenous copolymers. A possible cause of this apparent lack of detail was thought to be the occurrence of multiple scattering since Schelten and Schmatz[34] have shown in a theoretical study that this causes much detail to be lost from small-angle neutron scattering curves. Some support for this notion was found in our observation that while the amplitude of the main Bragg peak for the deuterated copolymers was increased (relative to their hydrogenous counterparts) the subsidiary Bragg maxima were less well-defined. In an attempt to clarify this point, we performed some experiments on copolymers with deuterated styrene blocks but with very thin specimens, <0.1 mm thick. No significant improvement in the resolution of the SPFF maxima was found. Another attempt to resolve the possibility of multiple scattering was the use of copolymer ABC1. This copolymer is only deuterated at the junction between the styrene and isoprene blocks, about five styrene units per molecule being deuterated. No improvement in the SPFF scattering was noted and consequently multiple scattering was not thought to be a source of any difficulty. Separate computer modeling studies of the scattered neutron intensity[35] have shown that the most likely source of this weak SPFF scattering is a distribution in size of the domains, severe effects being observed for comparatively modest size distributions.

Discussion

1. Comparison of Electron Microscopy with SANS. A comparison of the values of interdomain spacing and domain dimensions obtained by transmission electron microscopy with those of SANS shows that the values are the same magnitude for each technique. However, closer examination reveals that the agreement is best for the spherical systems and worst for the lamellar systems. Since the lamellar systems are considerably more ordered, as shown by SANS, and do not appear to be particularly prone to overstaining, this circumstance is somewhat surprising. The discrepancy is attributable to the severe dependence of TEM data on the orientation of the domains to the cutting edge of the microtome and the thickness of the slice obtained; this is particularly true for the lamellar domains. If these domains are not perfectly normal with respect to the cutting edge, then trapezoidal rather than rectangular lamellae result and the dimensions obtained depend on both cutting angle and thickness. This effect is apparent in the transmission electron micrograph, Figure 3a, where radically different spacing and thickness are observable in the same sample. For copolymers with spherical morphology these possible artifacts are absent and indeed this is reflected in the narrower spread in values in Table Ic. An additional possible source of error

Table VI
Volume Fractions of Styrene in Block Copolymers Determined Analytically (by UV Absorbance) and by Calculation from SANS Data

sample	volume fraction UV	volume fraction SANS
(a) Lamellar		
SI3	0.63	0.54
SI4	0.69	0.60
SI6	0.49	0.53
DSI7	0.42	0.48
DSI9	0.52	0.57
(b) Cylindrical		
SI2	0.32	0.36
SI5	0.84	0.81
SIS4	0.60	0.66
DSI5	0.77	0.79
DSI6	0.48	0.49
DSI10	0.37	0.44
(c) Spherical		
SI1	0.19	0.18
SIS1	0.14	0.15
SIS2	0.38	0.39
DSI1	0.28	0.28
DSIS1	0.10	0.09
ABC1	0.19	0.18

in the electron micrographs can arise in scooping the ultrathin films onto the grids; it is easy to stretch the film, with consequent deformation of the domains.

SANS, in which relatively thick samples, ~0.5 mm, with large sample areas are used, produces results that are more characteristic of the bulk copolymer and consequently is not so dependent on domain orientation since many domains are in the scattering volume.

2. Styrene Volume Fraction. A self-consistent check on the accuracy of the interdomain separation and the domain size is obtained by a comparison of calculated and experimentally determined volume fractions. Volume fractions of sytrene in the copolymers were calculated from SANS results by using the following formulas, obtained by a consideration of the domain packing assumed in interpreting the SANS diffraction profiles:

(a) lamellar morphology

$$\phi_S = L/d$$

(b) hexagonally close packed cylinders

$$\phi_S = 3.63(R_C/d)^2$$

(c) face-centered cubic arrangement of spheres

$$\phi_S = 5.92(R_S/d)^3$$

Table VI shows a selection of values calculated by these formulas and the volume fractions calculated from UV absorbance data. For these latter data the following homopolymer densities have been assumed to prevail in the copolymers: polyisoprene, 0.913 g mL^{-1}; polystyrene, 1.05 g mL^{-1}; deuteriopolystyrene, 1.13 g mL^{-1}.

The agreement between experimental and calculated volume fractions is very good, with a typical disagreement of 10% being apparent, but this is not disturbing when the possible variation in d and domain dimensions, is considered. Copolymers with spherical domain morphology have the greatest uncertainty in long-range structure, primarily due to the lack of detail in the SANS profiles. This type of calculation confirms our assignment of structure, since radically different values of ϕ_S would be obtained for a simple cubic arrangement of spheres, whereas a body-centered cubic arrangement produces styrene volume fractions which do not agree as closely with experimental values as those calculated on the basis of an fccub structure.

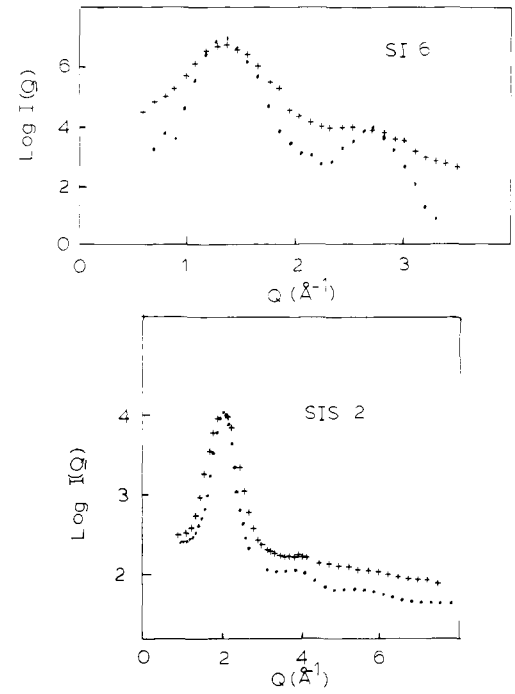

Figure 12. Influence of annealing on diffraction profiles of SIS2 and SI6: annealed (●); as cast (+). Both saamples were annealed at 150 °C under vacuum for 1 week.

3. Effect of Annealing on Morphology. In view of the lack of detail in the diffraction profiles for the copolymers with spherical morphology, attempts were made to improve this by annealing a few samples at 393 K under vacuum for an extended period. Diffraction profiles before and after this treatment are shown in Figure 12 for lamellar and spherical morphology block copolymers. In both cases the Q value of the peak maxima is not altered nor is there any evidence for additional "Bragg" peaks appearing. The general effect is a sharpening of the peaks and a small increase in the amplitude.

For truly crystalline substances a broadened "Bragg" peak is associated with the crystal thickness.[36] We interpret the narrowing of the peaks on annealing observed here as being due to a growth in the grain thickness and thus many more "lattice" planes being sampled by the neutron beam. While the grain thickness is calculable from the Scherrer formula,[36] absolute values are not reported here since the absolute resolution of the diffractometer depends on the Q range used, and hence the minimum resolvable thickness also is Q range dependent. This dependence can be removed by dividing the annealed grain thickness by the unannealed value; this approach indicates that the grain thickness doubles on annealing.

Apart from these copolymers with spherical domains, the other two types had diffraction maxima that were absent from the theoretically predicted pattern. A separate computer modeling study has shown that these absences are mainly due to minima in the SPFF coinciding with the "Bragg" maxima, thus causing a reduction in the intensity.

4. Theories of Domain Formation. Statistical thermodynamic theories of domain formation in block copolymers have been published by Meier[17] and Helfand and Wasserman.[18,19] While the detailed treatments differ in many respects, the physical basis used in both approaches is essentially identical. An equation for the free energy

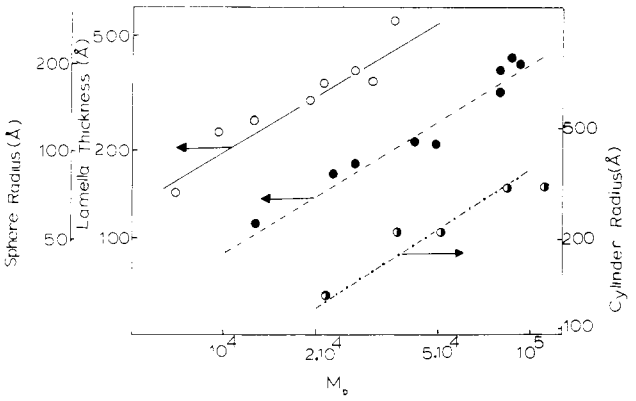

Figure 13. Domain dimensions as a function of domain molecular weight, M_D. Lines are calculated from the theory of Helfand while points are experimental data: lamellar morphology (- - -); cylindrical morphology (- · -); spherical morphology (—).

difference per molecule between a microphase-separated copolymer system and a homogeneous copolymer system is set up. This equation is then minimized with respect to the free energy, the domain separation being an adjustable parameter. There are three major components in the free energy equation, first, a surface free energy term, which is the driving force for domain growth, second, an entropy restriction to domain growth, arising from the placing of the junction between the two blocks at the domain–matrix boundary, and, third, an additional entropy limitation, due to the need to maintain uniform density in the separate phases. This latter restriction limits the chain configurations available to those that will alow the domain to be uniformly filled and limits domain growth due to the finite chain expansion available. The major difference between the two theories is in the assumption by Helfand and Wasserman that the interface at the domain boundary, where partial mixing of the two components takes place, is very small compared to the interdomain separation. This "narrow-interphase approximation" considerably simplifies the expression for the free energy difference, allowing the domain separation to be calculated directly by the minimization, in contrast to Meier's approach, which only allows direct calculation of the domain dimensions, the separation then being inferred from volume–packing relationships.

Meier[17] derives the relationships below between domain dimension and the molecular weight of the domain-forming component, M_D.

spheres

$$R_S = 1.33\alpha K M_D^{1/2}$$

cylinders

$$R_C = 1.00\alpha K M_D^{1/2}$$

lamellae

$$L = 1.4\alpha K M_D^{1/2}$$

where, α is the chain expansion factor, $K = (\langle r_0^2 \rangle / M)^{1/2}$, and $\langle r_0^2 \rangle$ is the mean square unperturbed end-to-end distance of the polymer molecule with molecular weight M.

Such explicit formulas are not written down by Helfand and Wasserman but values for R_S, R_C, and L may be calculated on the basis of their analysis using a FORTRAN program provided.[37] From such calculated values Helfand's analysis gives domain dimensions proportional to $M_D^{0.67}$. log–log plots of domain dimensions from SANS as a function of domain molecular weight are given in

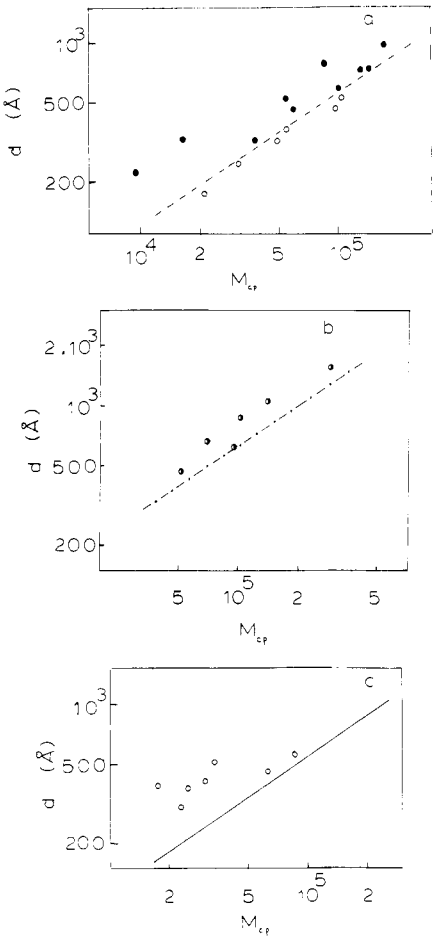

Figure 14. Interdomain separation as a function of total copolymer molecular weight, M_{CP}: (a) lamellar [(O) data from Hashimoto];[21] (b) cylindrical; (c) spherical.

Figure 13, which includes a line calculated from Helfand's theory over the same molecular weight range for each domain morphology.[39] Exact agreement with the theory is not obtained; however, the slopes obtained from best straight line fits to the data are in some agreement with the value of 0.67 predicted by Helfand. The relations obtained from these fits are

spheres

$$R_S = 0.89 M_D^{0.52}\ (\text{Å})$$

cylinders

$$R_C = 0.55 M_D^{0.56}\ (\text{Å})$$

lamellae

$$L = 0.22 M_D^{0.66}\ (\text{Å})$$

Since interdomain separation, d, and domain dimensions are connected through the volume fraction, the molecular weight exponent of d should have the same value as the domain dimensions. log–log plots of d as a function of copolymer molecular weight, M_{CP}, are shown in Figure 14, which also includes theoretical lines from the Helfand analysis. Clear differences are evident and best straight line fits to the data give the following relationships:

spheres

$$d = 8.6 M_{CP}^{0.36}\ (\text{Å})$$

cylinders

$$d = 0.32 M_{CP}^{0.67}\ (\text{Å})$$

lamellae

$$d = 0.997 M_{CP}^{0.56} \text{ (Å)}$$

Deviations from the theory of Helfand are not unexpected, since it is an equilibrium theory and the sample preparation is such that equilibrium conditions are probably not obtained. What is more surprising is the disparity between the molecular weight dependence of the domain separation and the domain size. A priori one expects that the domain size would display the greatest deviation from equilibrium behavior since attainment of equilibrium necessitates transport of block polymer between domains, a process that is unfavorable on thermodynamic and kinetic grounds (the latter especially so when the copolymer solutions are viscous). Added to this is the rather weak SPFF scattering from which the domain sizes are obtained, Figures 10 and 11. Consequently, deviations of domain size from theoretical predictions are not unexpected. A separate computer modeling study of block copolymer structure[35] and organization has produced reasons why gross deviations are not observed. It appears that neither a distribution in domain size about an average value (within limits) nor the absence of sharp phase boundaries influences the position of the maxima in the SPFF. Thus, provided they can be observed, these maxima will always be centered on the scattering vector determined by the domain size (i.e., the equilibrium domain size).

Such uncertainty should not be as evident in the domain separation since the "Bragg" peak is the dominant feature of the SANS scattering. Although domain size is a factor in determining separation distance, it is clearly not dominant here. Lamellar domains have only one dimension by which to adjust their dimensions whereas spherical domains have a choice of three dimensions. Consequently we would expect deviations from equilibrium predictions to increase from lamellar to spherical domains. This is not the case observed here since cylindrical systems are in good agreement with equilibrium theory. In this respect we note that annealing of samples under vacuum apparently produced no significant change in the interdomain distances, a growth in "grain" size apparently being the only observable affect.

The nonequilibrium domain separation may be due to domains becoming fixed in position at a certain point in the evaporation process, the approach to equilibrium thereafter being infinitely slow. Thermal annealing has no influence on this, although it appears that the "grains" in the copolymer grow indicating the presence of some movement in the systems. It was noted that after this annealing, the copolymers were no longer flexible but were hard, as though they were cross-linked. Consequently, the domains may have been "locked" into nonequilibrium positions by a cross-linking reaction. However, this type of mechanism is not reconcilable with the growth of grains after annealing and the origin of this disparity is still a source of investigation. Additionally, it must be pointed out that the molecular weight distributions of the copolymer samples studied here are greater than the monodisperse polymers assumed in the statistical thermodynamic theories of copolymer structure. Nonetheless, we fell that this polydispersity does not vitiate the comparisons made here.

5. Comparison with Other Studies. Detailed SAXS studies of styrene–isoprene block copolymers with spherical and lamellar domain morphology have been recently published by Hashimoto et al.[21,22] Much the same molecular weight range was studied; however, a major difference was the microstructure of the polyisoprene blocks, Hashimoto's having only 3% 1,4-addition microstructure. In reality direct comparison can only be made for lamellar morphologies, since SAXS specimens with spherical morphology related to polyisoprene spheres. Consequently, only the results for the lamellar morphologies are plotted for comparison. Our SANS data are higher over the whole range of molecular weight covered since the SAXS data are almost coincident with the equilibrium data from Helfand's theory. We can identify no clear reasons for this disparity since sample preparation conditions were similar for both SAXS and SANS samples, and the difference in microstructure is not thought to influence the molecular weight dependence of domain separation. This deviation from equilibrium values is especially suprising for the lamellar copolymers since these systems are able to approach equilibrium without mass transfer between domains by merely expanding or contracting the area of the lamellae.

Hadziioannou and Skoulios have published a series of papers[23] concerning mainly SAXS studies of lamellar styrene–isoprene di- and triblock copolymers. Here again a direct comparison cannot be made since these materials were oriented by subjecting to a shear gradient in the molten state. Consequently, the specimens have anisotropic properties and experimentally they found

$$d \propto M_{CP}^{0.79}$$

A similar approach to that detailed here has been used by Bates, Cohen, and Berney[38] on a SANS study of a styrene–butadiene diblock copolymer with spherical butadiene domains. Only one molecular weight was studied and they concluded that the domains were arranged in a body-centered arrangement.

Conclusions

For those copolymers with lamellar or cylindrical domains the long-range structure was assignable without ambiguity, whereas lack of detail in SANS diffraction profiles introduces some uncertainty for copolymers with spherical morphology. However, by comparison of experimental volume fractions with analytical values, it was concluded that a face-centered cubic arrangement of styrene domains prevails in those copolymers with a spherical domain morphology. Thermal annealing apparently has little influence on the detail in the diffraction profiles but results suggest that "grains" in the copolymer grow in size. Comparison of the SANS values of interdomain separation and domain size with the predictions of equilibrium theories shows that domain sizes agree well in both overall behavior and absolute values, while interdomain separation shows no such agreement. Possible sources for this disparity have been discussed and it appears to be a combination of nonattainment of equilibrium separation, a lack of sensitivity in the single-particle form factors, and the equilibrium assumption made in the statistical mechanical theories of domain formation.

The benefits of SANS in the study of block copolymers arise from the large scattering power of hydrogen nuclei. Typically, diffraction profiles were obtained by SANS experiments lasting <5 min, whereas earlier SAXS experiments[24] on the same specimens required up to 48-h exposure to obtain the same information. Furthermore, selective deuteration enables the contrast to be increased between particular features of the copolymer structure. The further advantages of this technique will be illustrated in later papers concerned with the interface between domains and the dimensions of blocks in domains. The results discussed here have provided useful comparison data for a model of block copolymer structure that embodies most of the features mentioned, i.e., long-range

arrangement of domains, distribution in domain size, and the nature and extent of the interface. The details and predictions of this model are the subject of a paper currently in preparation.[35]

Acknowledgment. We thank the Science and Engineering Research Council for financial support of this research. The assistance of our local contacts at the Institut Laue-Langevin, Drs. H. Haesslin and D. J. Cebula, is appreciated together with the assistance received at AERE Harwell from V. Rainey. We also thank Dr. E. Helfand for making available a preprint of his work and a listing of the FORTRAN program used.

Registry No. Styrene–isoprene copolymer, 25038-32-8; neutron, 12586-31-1.

References and Notes

(1) Thomas, D. A. *J. Polym. Sci., Polym. Symp.* **1977**, *No. 60*, 189.
(2) Guinier, A.; Fournet, G. "Small Angle Scattering of X-rays; Wiley: New York, 1955.
(3) Richards, R. W. In "Polymer Characterisation, Part 1"; Dawkins, J. V., Ed.; Applied Science Publishers: Essex, England, 1978.
(4) Maconnachie, A.; Richards, R. W. *Polymer* **1978**, *19*, 739.
(5) Higgins, J. S. *Treatise Mater. Sci. Technol.* **1979**, *15*.
(6) Ullman, R. *Annu. Rev. Mater. Sci.* **1980**, *10*, 261.
(7) See: *Faraday Discuss. Chem. Soc.* **1979**, *68*: Guenet, J. M.; Picot, C.; Benoit, H., 251. Stomm, M.; Fischer, C. W.; Dettenmaier, M.; Convert, P., 263. Ballard, P. H.; Burgess, A. N.; Crowley, T. L.; Longman, G. W.; Schelten, J., 279. Yoon, D. Y.; Flory, P. J., 288. Guttman, C. M.; Hoffman, J. D.; DiMarzio, E. A., 297.
(8) Folkes, M. J.; Keller, A. In "The Physics of Glassy Polymers"; Haward, R. N., Ed.; Applied Science Publishers: Essex, England, 1975.
(9) Manson, J. A.; Sperling, L. "Polymer Blends and Composites"; Plenum: New York, 1976.
(10) Noshay, A.; McGrath, J. E. "Block Copolymers: Overview and Critical Survey"; Academic Press: New York, 1977.
(11) Mayer, R. *Polymer* **1974**, *15*, 137.
(12) Douy, A.; Mayer, R.; Rossi, J.; Gallot, B. *Mol. Cryst. Liq. Cryst.* **1969**, *7*, 103.
(13) Hoffman, M.; Kampf, G.; Krömer, H.; Pampus, G. *Adv. Chem. Ser.* **1971**, *No. 99*, 351.
(14) Pedemonte, E.; Alfonso, G. C. *Macromolecules* **1975**, *8*, 85.
(15) Lewis, P. R.; Price, C. *Polymer* **1972**, *12*, 258.
(16) Gallot, B. R. M. *Adv. Polym. Sci.* **1978**, *29*, 85.
(17) Meier, D. J. *J. Polym. Sci., Part C* **1969**, *26*, 81; *Polym. Prepr., Am. Chem. Soc., Div. Polym. Chem.* **1970**, *11*, 400; **1974**, *15*, 171.
(18) Helfand, E. *Macromolecules* **1975**, *8* 552; **1976**, *9*, 879.
(19) Helfand, E.; Wasserman, Z. R. *Polym. Eng. Sci.* **1977**, *17*, 582; *Macromolecules* **1978**, *11*, 960, **1980**, *13*, 994.
(20) Leibler, L. *Macromolecules* **1980**, *13*, 1602.
(21) Hashimoto, T.; Shibayama, M.; Kawai, H. *Macromolecules* **1980**, *13*, 1237.
(22) Hashimoto, T.; Fujimura, M.; Kawai, H. *Macromolecules* **1980**, *13*, 1660.
(23) Hadziioannou, G.; Skoulios, A. *Macromolecules* **1982**, *15*, 258.
(24) Richards, R. W.; Thomason, J. L. *Polymer* **1981**, *22*, 581.
(25) Richards, R. W.; Thomason, J. L. *Polymer*, submitted for publication.
(26) Richardson, W. S.; Sacher, A. *J. Polym. Sci.* **1953**, *10*, 353.
(27) "Neutron Beam Facilities at the ILL", Institut Laue-Langevin, Grenoble, France, 1981.
(28) Baston, A. H.; Harris, D. H. C. "Neutron Beam Instruments at Harwell", HMSO, 1978.
(29) Ghosh, R. E. "A Computing Guide for Small Angle Scattering Experiments", ILL Report 81 GH 20T, 1981.
(30) Grubisic, Z.; Rempp, P.; Benoit, H. *J. Polym. Sci., Part B* **1967**, *5*, 753.
(31) Runyon, J. R.; Barnes, D. E.; Rudd, J. F.; Tung, L. H. *J. Appl. Polym. Sci.* **1969**, *13*, 2359.
(32) Tung, L. H. *J. Appl. Polym. Sci.* **1979**, *24*, 953.
(33) Korstorz, G. *Treatise Mater. Sci. Technol.* **1979**, *15*.
(34) Schelten, J.; Schmatz, W. *J. Appl. Crystallogr.* **1980**, *13*, 385.
(35) Richards, R. W.; Thomason, J. L., to be published.
(36) Cullity, B. D. "Elements of X-ray Diffraction"; Addison-Wesley: New York, 1970.
(37) Helfand, E.; Wasserman, Z. R. In "Developments in Block Copolymers"; Goodman, I., Ed.; to be published.
(38) Bates, F. S.; Cohen, R. E.; Berney, C. V. *Macromolecules* **1982**, *15*, 584.
(39) It should be noted that the molecular weight dependence of domain size predicted by this theory is the same whether the domains are of isoprene or styrene; i.e., it is immaterial which part of the phase diagram is explored so long as the same domain morphology is obtained. This does not mean to say that the domains of polyisoprene and polystyrene will have the same size and separation for the same molecular weights; the differences are, however, negligibly small.

A Fluorescence Method To Determine the Solubility Parameters δ_H of Soluble Polymers at Infinite Dilution. Cyclization Dynamics of Polymers. 11

Xiao-Bai Li,† Mitchell A. Winnik,* and James E. Guillet

Lash Miller Laboratories, Department of Chemistry and Erindale College, University of Toronto, Toronto, Ontario, Canada M5S 1A1. *Received September 17, 1982*

ABSTRACT: A polystyrene sample was prepared containing pyrene groups spaced at regular intervals along the chain backbone. Fluorescence studies of this polymer in dilute solution showed both pyrene (I_M) and pyrene excimer (I_E) fluorescence. The ratio of these fluorescence intensities, I_E/I_M, varied sensitively with a change in solvent. One effect is due to solvent viscosity η_0. A plot of $\eta_0(I_E/I_M)$ against the Hildebrand solubility parameter δ_H gave two straight lines intersecting at $\delta_H = 9.1$. This is the δ_H value reported in the literature for polystyrene. A new technique based upon these observations for using fluorescence spectroscopy to determine δ_H for polymers is described.

Introduction

The solubility parameter concept based on regular solution theory has been used extensively in practical applications of polymers in various solvents and solvent mixtures. It has proven to be a valuable empirical tool in both laboratories and industries.

The solubility parameter, δ_H (units of $(cal/cm^3)^{1/2}$), for any compound is defined from Hildebrand–Scatchard solution theory as the square root of the cohesive energy density, which is itself defined as the ratio of the energy of vaporization, ΔE_v, to the molar volume, V_1, both referred to the same temperature (eq 1).

$$\delta_H \equiv (\Delta E_v / V_1)^{1/2} \quad (1)$$

†On leave from Nankai University, Tianjin, China; deceased April 1983.

0024-9297/83/2216-0992$01.50/0